# Hybrid AG-FFPI/RLPFG for Simultaneously Sensing Refractive Index and Temperature

Cheng-Ling Lee, *Member, IEEE*, Wen-Fung Liu, Zi-Yu Weng, and Fu-Chih Hu

***Abstract*—This work presents a novel, simple, and sensitive device for simultaneously sensing refractive index (RI) and temperature ($T$) of its surrounding environment. The sensing elements are based on a hybrid air-gap fiber Fabry–Pérot interferometer (AG-FFPI) with a reflective long-period fiber grating (RLPFG). An air gap of around 10 $\mu$m is formed in an Sn-overlaying process on the fiber endface to make a fiber Fabry–Pérot interferometer whose interferometric cavity is formed between the fiber endface and the surface of the Sn metal. The proposed devices are characterized by the simple fabrication and high sensitivity to both $T$ and RI, which can be simultaneously measured. Additionally, the proposed device can readily recognized the response from ambient variations in $T$ or the RI.**

***Index Terms*—Air-gap fiber Fabry–Pérot interferometer (AG-FFPI), fiber-optics component, fiber sensors, long-period fiber grating (LPFG).**

## I. Introduction

THE simultaneous measuring, monitoring, or sensing of many parameters of a system is of scientific and technological importance. Various all-fiber interferometers that incorporate fiber gratings (FGs) have been developed with numerous smart and hybrid structures for a wide range of potential applications in bio-sensing, chemical sensing, and the sensing of various other physical parameters. Various works have focused on enhancing measurement sensitivity and the simultaneous sensing of several parameters [1]–[9]. Because the LPFGs are well known to be sensitive to the ambient variations, therefore most of the smart sensing schemes are based on the LPFGs; for example, an LPFG may incorporates a fiber Bragg grating (FBG) to support hybrid measurements schemes [1], [2]; and a concatenated structure of the multiple LPFGs can support a sensing method that is based on the cladding and core mode interference mechanism [3]–[5]. Another configuration involves a mirror that is coated on the endface of an LPFG and an intrinsic AG-FFPI [6], while another involves an FBG that is incorporated into a low-finesse Fabry–Pérot interferometric cavity that is formed by coating a monolayer material on the fiber endface [7]. In [6], Kim *et al.* firstly introduced a RLPFG that incorporated an AG-FFPI to measure simultaneously RI and $T$. The air gap inside the fiber was formed by hydrofluoric acid etching, which was difficult to control and complicated to be implemented. Similarly, a Fabry–Pérot cavity that is formed by using the electrostatic self-assembled monolayer process for molecular deposition to form a humidity-sensitive coating on the end of a fiber would difficult to be fabricated [7].

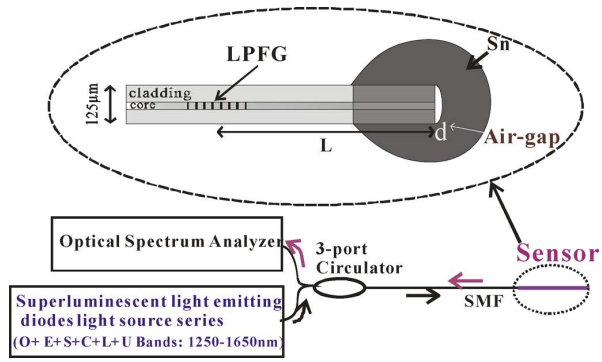


Fig. 1. Configuration of the hybrid AG-FFPI/RLPFG sensor.

In this Letter, we have presented a novel, simple, cost-effective and sensitive device for simultaneously sensing external RI and $T$. The sensing configuration is based on a hybrid AG-FFPI with an integrated RLPFG. By skillfully overlay the metal Sn over one endface of LPFG, an air gap can be formed between the surface of the metal Sn and the end of the fiber. This gap can be formed the Fabry–Pérot cavity. The proposed devices have the advantages, such highly sensitivity for simultaneously sensing both $T$ and RI. More importantly, it can readily capture ambient variation in the surrounding $T$ or the RI.

## II. Sensor Configuration and Principle of Operation

This study presents for the first time a very simple, cost-effective fiber sensor whose structure is based on a RLPFG integrated with an AG-FFPI made by the Sn-overlaying on one endface of the RLPFG with a fiber arm of $L = 7$ cm, forming a hybrid air-gap fiber interferometer/reflective long-period fiber grating (AG-FFPI/RLPFG) device is shown in Fig. 1. The interference mechanism in the AG-FFPI is based on the two-beam interference of the low-fineness air-gap Fabry–Pérot cavity [6]. Metal Sn (Tin) can be easily processed because of its low melting point (231.9 °C) and it is also a good electrical/thermal conductor. It is therefore extensively adopted in the electrical and electronics industries. Therefore, in this work, when the fiber endface was inserted into an extremely small drop of melting Sn, an air gap was naturally formed between the fiber and the

Manuscript received March 14, 2011; revised May 24, 2011; accepted May 28, 2011. Date of publication July 18, 2011; date of current version August 10, 2011. This work was supported in part by the National Science Council of the Republic of China under Grant NSC 98-2221-E-239-002-MY2.

C.-L. Lee, Z.-Y. Weng, and F.-C. Hu are with the Department of Electro-Optical Engineering, National United University, Miaoli 360, Taiwan (e-mail: cherry@nuu.edu.tw).

W.-F. Liu is with the Department of Electrical Engineering, Feng Chia University, Taichung 407, Taiwan (e-mail: wfliu@fcu.edu.tw).

Color versions of one or more of the figures in this letter are available online at http://ieeexplore.ieee.org.

Digital Object Identifier 10.1109/LPT.2011.2158816

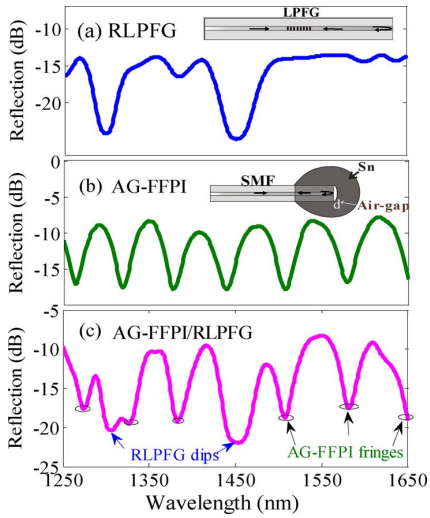


Fig. 2. Experimental reflection spectra of (a) LPFG in air before Sn-overlaying, (b) SMF endface with Sn-overlaying to form a simple AG-FFPI, and (c) the proposed hybrid AG-FFPI/RLPFG that is formed by combining devices in (a) and (b).

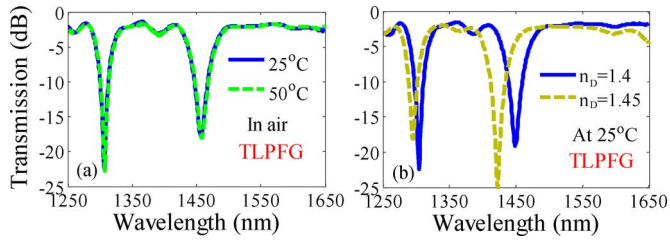


Fig. 3. Experimental transmission spectra of general TLPFG for the measurements with different (a) surrounding $T$ and (b) external RI.

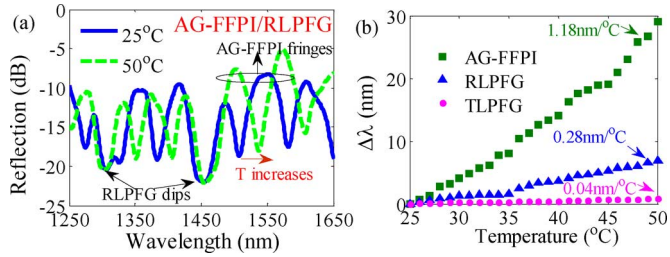


Fig. 4. (a) Experimental spectra of the proposed hybrid AG-FFPI/RLPFG with various $T$; (b) $\Delta\lambda$ of the dips of AG-FFPI, RLPFG, and TLPFG as a function of surrounding $T$ in the air.

metal Sn owing to the cohesion of the bulk Sn. Based on our experiences, by carefully controlling the inserting time of the fiber, the air–gap length would be dominated substantially. In general, faster inserting time would obtain a smaller air-gap before the melting Sn becomes into solid. We can successfully fabricate the air-gap within the range of around $8 \sim 31$ $\mu$m by using the above method with the repeatability greater than 90% so far, but cannot precisely quantize the inserting time with the function of the air-gap distance. The reflection spectra of an RLPFG with a grating period of $\Lambda = 300$ $\mu$m, grating length of 1 cm and the interference fringes that are generated by the AG-FFPI of a single mode fiber (SMF) are measured using an optical spectrum analyzer (OSA), and displayed in Fig. 2(a) and (b), respectively. From Fig. 2(a), the dip of RLPFG is broader than that of TLPFG, and the loss is high, approximately 15 dB, since the endface of the interface surfaces with Fresnel reflection is merely $R \sim 0.034$. As shown in Fig. 2(b), a sinusoidal spectrum of the interference fringes caused by the air gap was obtained. In the Fig. 2(b), the loss from an SMF fiber endface that is overlaying with Sn is smaller, averaging about 8.5 dB, owing to the reflection ($R \sim 0.5$) from the Sn metal is increased. The reflection spectrum with a maximum extinction ratio of around 9 dB is obtained from the proposed AG-FFPI configuration. The two above structures can be combined to realize hybrid AG-FFPI/RLPFG sensor and obtain the optical spectrum that is shown in Fig. 2(c). Fig. 2(c) displays a superposition of spectral responses from both of the RLPFG and the AG-FFPI structures and spectrum also indicates the locations of the AG-FFPI interference fringes and the resonant peaks of RLPFG, respectively.

For a conventional transmission LPFG (TLPFG) with a grating period of 300 $\mu$m and a grating length of 1 cm, written on an SMF, the transmission spectra measured from the variation in the surrounding $T$ and the external RI ($n_{ext}$) are shown in Fig. 3(a) and (b), respectively. Fig. 3(a) demonstrates that the TLPFG is insensitive to $T$, such that a very little wavelength shift ($\Delta\lambda$) toward longer wavelengths occurs as $T$ is increased because the changes with the $T$ of the differential effective index of the core and cladding modes and in the grating periodicity are very small [8]. On the other hand, the shift of the wavelength dips is obtained toward the shorter wavelength side as the $n_{ext}$ is increased (Fig. 3(b)).

## III. Results and Discussion

Although the parametric sensitivity of the LPFG exceeds those of FBG sensors, it can be further increased by the use of smart configurations or hybrid structures. To demonstrate the effective sensing performance of the proposed AG-FFPI/RLPFG sensor with the hybrid configuration, this sensor is utilized in surrounding $T$ and external RI sensing applications. The sensor was placed on a TE cooler inside a closed space with the $T$ (°C) increased from 25 °C to 50 °C. Fig. 4(a) shows the measured reflection spectra of the AG-FFPI/RLPFG, which shifts toward the longer wavelength side as $T$ is increased. The shift for the AG-FFPI interference fringes is much larger than those of the RLPFG and the TLPFG (Fig. 3(a)). Fig. 4(b) plots the tuning efficiency and the $\Delta\lambda$ of the fringes of the AG-FFPI, the RLPFG and the TLPFG as functions of surrounding temperature in air. From the experimental results, the sensitivity of the proposed RLPFG (0.28 nm/°C) to the $T$ is about seven times that of the TLPFG (0.04 nm/°C) and that of the presented AG-FFPI (1.18 nm/°C) is almost 30 times that of the TLPFG. Since the thermal expansion coefficient of metal Sn $\sim 2.2 \times 10^{-5}$°C$^{-1}$ is about 40 times greater than that of the silica fiber ($\sim 5.5 \times 10^{-7}$°C$^{-1}$), thus the $T$ sensitivity of the sensor is dominated by the Sn. Fig. 5(a) presents the reflection spectra of the proposed AG-FFPI/RLPFG that are obtained to measure the external RI ($n_{ext}$). The main $\Delta\lambda$ are observed in the dips of the RLPFG, which is highly sensitive to $n_{ext}$. However, AG-FFPI interference fringes are almost independent of the surrounding $n_{ext}$. Fig. 5(b) plots the shift $\Delta\lambda$ at 1450 nm resonant dip of the TLPFG (Fig. 3(b)) and the proposed RLPFG as a function of the RI of the surroundings. The $\Delta\lambda$ of the RLPFG slightly exceeds that of the TLPFG at a given surrounding $n_{ext}$, and the $\Delta\lambda$ of the AG-FFPI fringes

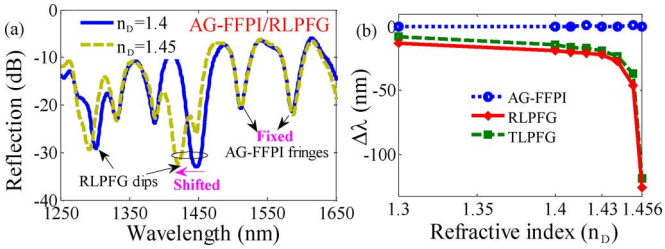


Fig. 5. (a) Experimental spectra of the proposed hybrid AG-FFPI/RLPFG at different surrounding $n_{ext}$ at 25 °C, (b) $\Delta\lambda$ at 1450-nm resonant dips of the TLPFG and the RLPFG as a function of the RI. The shifts are measured with corresponding to the dip at $n_D = 1.0$ (air). $n_D$ means the $n_{ext}$ is measured at the sodium $D$ line (589.3 nm).

is almost zero. The RLPFG is more sensitive because the optical light propagates twice through the LPFG with longer optical path difference, resulting in a small larger $\Delta\lambda$. Most importantly, the proposed measured configuration can easily determine the $\Delta\lambda$ from the spectra that is caused by variations of the $T$ or the $n_{ext}$.

The $\Delta\lambda$ value both from the RLPFG and the AG-FFPI caused by a change in $T$ or $n_{ext}$ can be respectively estimated by using the following equations.

$$\frac{\Delta\lambda_{RLPFG}}{\lambda_{RLPFG}} = \left[\frac{1}{\Delta n_{eff}}\frac{\partial(\Delta n_{eff})}{\partial T} + \frac{1}{\Lambda}\frac{\partial(\Lambda)}{\partial T}\right]\Delta T + \left[\frac{1}{\Delta n_{eff}}\frac{\partial(\Delta n_{eff})}{\partial n_{ext}}\right]\Delta n_{ext} = A\Delta T + B\Delta n_{ext} \quad (1)$$

$$\frac{\Delta\lambda_{AG-FFPI}}{\lambda_{AG-FFPI}} = \frac{1}{d}\frac{\partial d}{\partial T}\Delta T = C\Delta T \quad (2)$$

where $\Delta n_{eff}$ is the difference between the effective indices of the core mode and the cladding mode. The coefficients $A$, $B$, and $C$ can be determined by measuring the dip responses of the sensors with the variations in $T$ and $n_{ext}$. The corresponding sensitivity from the matrix coefficients are about 0.275 nm/°C, $-260$ nm/RIU within a linear range $n_{ext} = 1.4 - 1.44$ and 1.175 nm/°C, respectively. Therefore, the following equation, (3), obtained by combining (1) and (2) enables the proposed AG-FFPI/RLPFG to be used to measure the $n_{ext}$ and $T$ simultaneously.

$$\begin{pmatrix}\Delta T\\ \Delta n_{ext}\end{pmatrix} = \begin{pmatrix}A & B\\ C & 0\end{pmatrix}^{-1}\cdot\begin{pmatrix}\frac{\Delta\lambda_{RLPFG}}{\lambda_{RLPFG}}\\ \frac{\Delta\lambda_{AG-FFPI}}{\lambda_{AG-FFPI}}\end{pmatrix} = \begin{pmatrix}0.275 & -260\\ 1.175 & 0\end{pmatrix}^{-1}\cdot\begin{pmatrix}\Delta\lambda_{RLPFG}\\ \Delta\lambda_{AG-FFPI}\end{pmatrix}. \quad (3)$$

The $T$ sensitivity of 0.275 nm/°C of our RLPFG is 2~3$ times greater than a correct estimation of the sensitivity for a TLPFG $\sim 0.098$ nm/°C reported in [8]. It is because that the proposed RLPFG is operated in the reflective mode with a very long propagating $L = 7$ cm which would increase the shifts [6]. It is also verified by the cascaded (dual) LPFGs having greater sensitivity [5]. The sensitivity of the $n_{ext}$ of LPFG depends on the cladding mode order and also varies with fiber types. An exact estimate based on the coupled-mode theory [10] determined the sensitivity $n_{ext}$ of LPFG is about $-262.5$ nm/RIU within $n_{ext} = 1.4 - 1.44$ and very similar to that of the RLPFG. Even so, the total $\Delta\lambda$ of RLPFG slightly greater than that of TLPFG within the entire measurement with several nm. It is worth to mention that the novel Sn-overlaying AG-FFPI incorporated in the structure can greatly enhance the $T$ sensitivity and not be affected by $n_{ext}$ of the surrounding. By using an approach in [9], the maximum errors for the measurements of the $T$ and $n_{ext}$ are respectively 1.56°C and 2.43 $\times 10^{-3}$ RIU and the rms errors are respectively 1.33°C and 1.51 $\times 10^{-3}$ RIU for our sensor within the ranges $n_{ext} = 1.4 - 1.44$ and $T = 25 - 50$°C. The main drawback of the sensor is an overlap of the wavelength dips can occur, thus limits the measured range. From the experimental results, the $T$ range of the measurement of merely about 25–85°C with high sensitivity of 1.175 nm/°C and the RI measurement range with $n_D = 1 - 1.45$ are achieved by the proposed sensor under an identifiable shifts of the wavelength dips.

## IV. Conclusion

This work demonstrated a new, cost-effective, simple and sensitive hybrid structure, which was fabricated by incorporating an RLPFG with an AG-FFPI. Experimental results demonstrated that the proposed sensor can simultaneously measure the RI and the $T$ of the surroundings, corresponding to the $\Delta\lambda$ in the spectral response of the sensor to the change in $T$ or RI can be easily identified. The $T$ sensitivity of the hybrid AG-FFPI/ RLPFG is approximately 30 times greater than that of the conventional silica-based TLPFG. This device can provide the advantages of simplicity, easy fabrication, high sensitivity, and has the capability to simultaneously measure various physical parameters for applying in a wide range of sensing systems.

## References

[1] X. Shu, B. A. L. Gwandu, Y. Liu, L. Zhang, and I. Bennion, "Sampled fiber Bragg grating for simultaneous refractive-index and temperature measurement," *Opt. Lett.*, vol. 26, pp. 774–776, 2001.

[2] X. Chen, K. Zhou, L. Zhang, and I. Bennion, "Simultaneous measurement of temperature and external refractive index by use of a hybrid grating in *D* fiber with enhanced sensitivity by HF etching," *Appl. Opt.*, vol. 44, pp. 178–182, 2005.

[3] A. P. Zhang, L. Y. Shao, J. F. Ding, and S. He, "Sandwiched long-period gratings for simultaneous measurement of refractive index and temperature," *IEEE Photon. Technol. Lett.*, vol. 17, no. 11, pp. 2397–2399, Nov. 2005.

[4] J. Yan, A. P. Zhang, L. Y. Shao, J. F. Ding, and S. He, "Simultaneous measurement of refractive index and temperature by using dual long-period gratings with an etching process," *IEEE Sensors J.*, vol. 7, pp. 1360–1361, 2007.

[5] B. A. L. Gwandu, X. Shu, T. D. P. Allsop, W. Zhang, L. Zhang, I. Bennion, and I. Bennion, "Simultaneous refractive index and temperature measurement using cascaded long-period grating in double-cladding fibre," *Electron. Lett.*, vol. 38, pp. 695–696, 2002.

[6] D. W. Kim, F. Shen, X. Chen, and A. Wang, "Simultaneous measurement of refractive index and temperature based on a reflection-mode long-period grating and an intrinsic Fabry–Perot interferometer sensor," *Opt. Lett.*, vol. 30, pp. 3000–3002, 2005.

[7] F. J. Arregui, I. R. Matías, K. L. Cooper, and R. O. Claus, "Simultaneous measurement of humidity and temperature by combining a reflective intensity-based optical fiber sensor and a fiber Bragg grating," *IEEE Sensors J.*, vol. 2, no. 5, pp. 482–487, 2002.

[8] V. Bhatia, "Applications of long-period gratings to single and multi-parameter sensing," *Opt. Express*, vol. 4, pp. 457–466, 1999.

[9] X. Bao, Q. Yu, and L. Chen, "Simultaneous strain and temperature measurements with polarization-maintaining fibers and their error analysis by use of a distributed Brillouin loss system," *Opt. Lett.*, vol. 29, pp. 1342–1344, 2004.

[10] K. -W. Chung and S. Yin, "Analysis of a widely tunable long-period grating by use of an ultrathin cladding layer and higher-order cladding mode coupling," *Opt. Lett.*, vol. 29, pp. 812–814, 2004.